Monte Carlo Simulation of Two ^{106}Ru Eye Plaques in a New Mathematical Human Eye Model

Original Article

Ali Asghar Mowlavi, Majed Yazdani

Physics Department, Sabzevar Tarbiat Moallem University, Sabzevar, Iran.

(Received 27 July 2008, Revised 15 October 2008, Accepted 26 October 2008)

ABSTRACT

BEBIG Ruthenium-106 ophthalmic plaques have been used for treatment of uveal melanoma, retinoblastoma, melanoma of the iris and other special applications for many years. The plaques consist of a thin film of ^{106}Ru, a beta emitter, encapsulated in pure silver. The present work proposes a new mathematical eye model for ophthalmic brachytherapy dosimetry. This new model includes detailed description of internal structures, allowing dose determination in different regions of the eye for a more adequate clinical analysis. In the present work, we have used MCNP4C code to calculate relative dose in a new human eye model. The isodose curves and dosimetric characteristics for two ^{106}Ru eye applicators have been determined. Also, absorbed dose values due to both small CCA and CCB concave applicators were obtained for each one of the different structures which compose the eye model and can give relevant information in eventual clinical analyses.

Key words: ^{106}Ru eye plaque, Dose calculation, Mathematical human eye model, MCNP4C code

Iran J Nucl Med 2008; 16(2): 16-22

Corresponding author: Ali Asghar Mowlavi, Department of Physics, Sabzevar Tarbiat Moallem University, Sabzevar, Iran.
E-mail: E-mail: amowlavi@stt.ac.ir

INTRODUCTION

Theoretical and experimental dosimetric studies have led to useful information on the dependence of the brachytherapy source geometry and materials. Usually, Monte Carlo method has been used to define dose distribution function, the radial dose variation, and the dose calculation close to the source in brachytherapy (1). Brachytherapy using removable ophthalmic plaques is a convenient alternative to enucleation for the treatment of malignant melanoma, or other tumors of the eye (2). The choice of the most adequate plaque for each specific treatment depends mainly on the height of the tumor apex. Medium- and large-sized tumors are usually treated with ^{103}Pd or ^{125}I applicators, whereas for small-sized tumors β-ray applicators of ^{106}Ru or ^{90}Sr are preferred. In particular, choroidal melanomas can be successfully treated with applicators containing the β-emitting nuclide ^{106}Ru. Ample experience in the use of this kind of treatment has been accumulated for more than 25 years and the number of hospitals using this method is still increasing (3-5). Although different types of eye applicators are available, the most commonly used are the CCA and CCB concave applicators.

Usually, the eye anatomy is represented by a simple sphere with the presence of few distinct structures (6, 7). However, sometimes distinct dose determination in different regions of the eye is needed for a more adequate clinical analysis. Taking into account this fact, a detailed geometric model of the human eye, including the choroid, retina, sclera, lens, cornea, anterior chamber, vitreous humour and optic nerve has been developed (8). For calculating the effect of source shield or applicators and dose distribution usually Monte Carlo codes as MCNP, EGS4, GEANT4 are applied. In this present work, we have used MCNP4C code (9) to calculate amount of dose in a new eye phantom.

METHODS

Ophthalmic applicators

The radioactive nucleus ^{106}Ru disintegrates to the stable nuclide ^{106}Pd via ^{106}Rh. The half-life of ^{106}Ru is 368.2 days and for ^{106}Rh, which mainly contributes to the β-particle emission, the half-life is 29.9 s. The electron spectrum of ^{106}Ru has a maximum energy of 39.4 keV, whereas in case of disintegration of ^{106}Rh the mean energies of the continuous β-particle spectra for the three transitions with the highest yields are 1.51 MeV (79%), 0.97 MeV (9.7%) and 1.27 MeV (8.4%), with a maximum energy of 3.5 MeV (10). Sánchez-Reyes et al. have considered only the three β-transitions of the ^{106}Rh nuclear decay in their computational dosimetry (11). But, we consider the real beta spectra of ^{106}Ru and ^{106}Rh in our simulation (Figure 1).

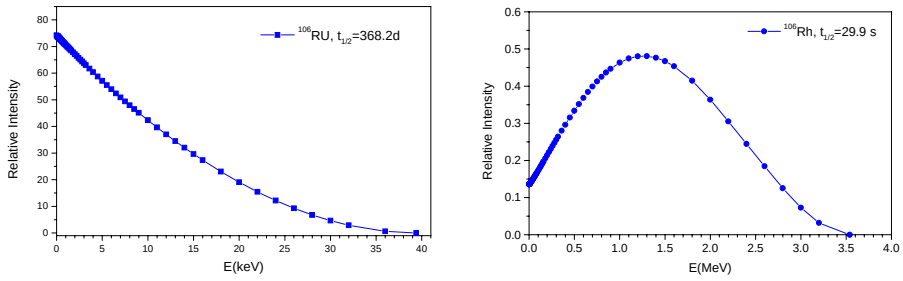

Figure 1: The beta spectra of ^{106}Ru and its daughter, ^{106}Rh.

In the present study we consider the CCA and CCB concave applicators, with a radius of curvature of 12 mm and external diameters of 15.5 and 20 mm, respectively (11). They consist of two sealed concentric spherical foils of silver with the radioactive substance placed between them (see Figure 2). These applicators are produced by Bebig Isotopentechnik und Umweltdiagnostik in Germany (11).

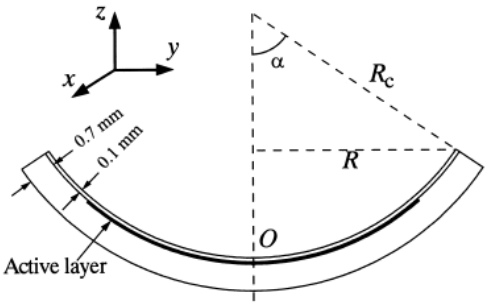

Figure 2: Schematics of the geometry used in the simulations. The radial scale of the applicator is enlarged for clarity and the active layer, which has a negligible thickness, is indicated. Notice that the origin of the reference frame is placed at the centre of the surface O and the rotational symmetry of the system about the z-axis.

In the simulations, the geometry specifications given by the manufacturer have been strictly followed (Figure 2). The volume of each silver foil is limited by two concentric spherical sectors and a cone of aperture α-arccos (R/R_c), where R and R_c are the external radius of the applicator and the curvature radius of the inner surface, respectively. The laboratory reference frame used in the simulations has its origin at the centre of the applicator inner surface, with the symmetry axis as the z-axis. The centre of curvature of the applicator is 1.2 cm from the inner surface. We have assumed that the active radionuclide ^{106}Ru is uniformly distributed on the spherical interface between the backing and window silver foils. The outer radius of the active area is smaller than the applicator radius, i.e. 0.5 cm for the CCA and 1.0 cm for the CCB, according to the manufacturer's specifications.

The eye and tumor anatomy

The eye anatomy is composed of three layers enclosing the eye body, namely the retina (inner), choroids (middle) and the sclera (outer). According to the ICRP 23 (12) the total weight of both eyes is 15 g. Both sclera and choroid are 1 mm thick on average. The critical parts for vision are the retina, optic nerve and disc, macula and lens. The cornea is a transparent structure formed by a segment of spherical shell and permits the passage of light. The lens is a transparent biconvex body with no blood supply and particularly vulnerable to radiation. Its germinative zone has a high mitotic activity, being considered as the origin of the radiation-induced cataracts (13). The sclera is important to protect the intra-ocular contents and optic integrity and to avoid deformation of the eyeball. Some of the eye cancer treatments based on ophthalmic applicators reported in the literature are the malignant melanoma of the choroid, retinoblastoma and the posterior uveal melanoma (14–18). Tumor volumes assume different sizes and shapes and can be classified into three categories: small tumours, which sizes are <400 mm^3, medium-sized tumours, ranging from sizes of 400 to 1000 mm^3 and large tumours, with sizes over 1000 mm^3. Basically, for simulation purpose the tumor volumes are represented by a semi-ellipsoid located in some part of the eyeball (8).

Mathematical model of eye and tumor

The mathematical model of the eye and its components are described by the following equations:

Sclera, choroid and retina: The sclera, choroid and retina have been defined as three concentric spherical shells, which are ~1 mm thick, according to the expression:

$$(R_i - 0.1)^2 \le (x)^2 + (y+1.6)^2 + (z)^2 \quad [1]$$

Where i = 1, 2, 3; R_1 = 1.20 cm for sclera; R_2 = 1.11 cm for choroid; and R_3 = 1.01 cm for retina.

Tumour: The tumor has been defined as an ellipsoid cut by the spherical surface of sclera forming a semi-ellipsoid which is situated inside the inner most part of the eye:

$$\begin{cases} 0.444(x)^2 + 0.04(y-3.6)^2 + 0.444(z)^2 \le 1 \\ (x)^2 + (y+1.6)^2 + (z)^2 \le 1.20^2 \end{cases} \quad [2]$$

Cornea: The cornea is an elliptical shell limited by two concentric ellipses and the outer spherical surface of the sclera:

$$\begin{cases} 1.56(x)^2 + 1.62(y+1.6)^2 + 1.66(z-0.73)^2 \ge 1 \\ 1.29(x)^2 + 1.39(y+1.6)^2 + 1.52(z-0.73)^2 \le 1 \\ (x)^2 + (y+1.6)^2 + (z)^2 \ge 1.20^2 \end{cases} \quad [3]$$

Optic nerve and wall: The optic nerve and wall are represented, respectively, by a cylinder and a cylindrical shell, concentrically placed, which extend from the outer sclera surface to plane $y \le 3$:

$$\begin{cases} (x)^2 + (z)^2 \le 0.35^2 \\ (x)^2 + (z)^2 \ge 0.40^2 \\ (x)^2 + (y+1.6)^2 + (z)^2 \ge 1.20^2 \\ y \le 3 \end{cases} \quad [4]$$

The cylinders are rotated by 30° in relation to the coordinate system.

Lens: The lens is formed by the region surrounded by two surfaces: the spherical surface of the sclera and the elliptical surface given by:

$$\begin{cases} 2.98(x)^2 + 2.98(y+1.6)^2 + 9.15(z-0.73)^2 \le 1 \\ (x)^2 + (y+1.6)^2 + (z)^2 \le 1.20^2 \end{cases} \quad [5]$$

Anterior chamber: The anterior chamber is the geometric region between the surface that defines the inner wall of the cornea and the outer surface of the sclera:

$$\begin{cases} 1.56(x)^2 + 1.62(y+1.6)^2 + 1.66(z-0.73)^2 \le 1 \\ (x)^2 + (y+1.6)^2 + (z)^2 \ge 1.20^2 \end{cases} \quad [6]$$

Vitreous body: The vitreous body is the spherical region limited by the inner surface of the retina. Most part of the tumor is modeled as being located inside this region:

$$(x)^2 + (y+1.6)^2 + (z)^2 \le 0.935^2 \quad [7]$$

The complete geometric model of the eye including the tumor region is shown in Figure 3. Soft tissue composition that used in this work, are listed in Table 1 (1). Mass density for soft tissue is 1.04 g/cm^3. Table 2 shows the masses of each eye phantom component.

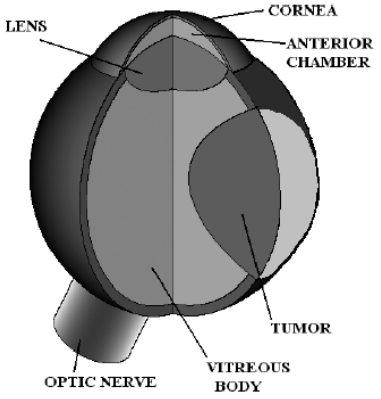

Figure 3: Geometric model of the eye phantom.

Table 1: Soft tissue composition and mass density for soft tissue used in MCNP input

Element	Weight Fraction	Element	Weight Fraction
H	10.454	S	0.204
C	22.663	Cl	0.133
N	2.490	K	0.208
O	63.525	Ca	0.024
Na	0.112	Fe	0.005
Mg	0.013	Zn	0.003
Si	0.030	Rb	0.001
P	0.134	Zr	0.001

Table 2: Masses of the various eye components in grams

Eye component	Mass (g)	
	This work	ICRP 23
Vitreous body	2.946	3.90
Retina	0.927	
Choroid	1.470	
Sclera	1.570	1.02 1.33
Tumour	1.011	
Cornea	0.180	0.18
Anterior chamber	0.352	0.15 0.35
Lens	0.202	0.20

RESULTS AND DISCUSSION

The Monte Carlo *N*-Particle code (MCNP version 4C) with photon cross-section library DLC-200 was used for the dose rate simulations (9). In the present work, dose calculations have been performed utilizing the Monte Carlo code MCNP-4C using ^{106}Ru plaques by using tally *F8:e of MCNP code (9). We used just 1keV cut off of electron energy in our calculations, other variance reduction techniques are not allowed for F8:e tally.

Figure 4 shows the relative dose profile calculated for the ^{106}Ru source applicator along its central axis in the water phantom compared with the result provided by the manufacturer. Along the central axis with 0.4 mm step, relative dose curves have been calculated. Deposited energy in the above eye phantom's components per one particle of source is shown in Table 3. We must mention that the relative errors in our calculations are less than 1%.

Simulation of the new mathematical human eye model by MCNP code is very useful to evaluate absorbed dose in any section of human eye, accurately.

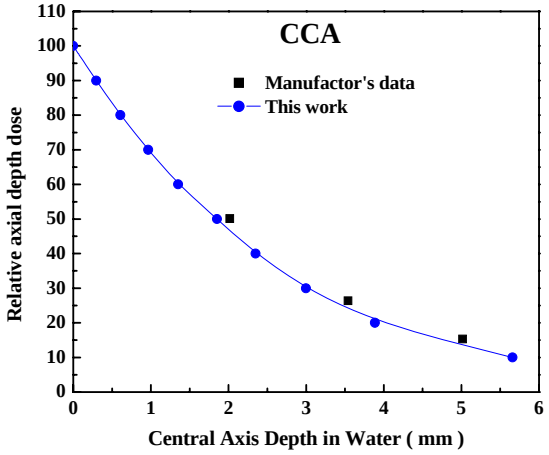

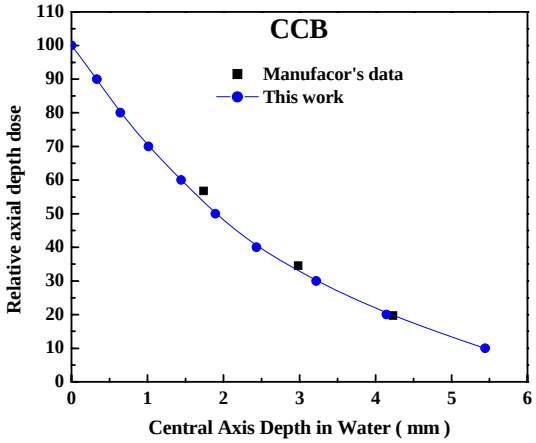

Figure 4: Depth dose (along the central axis) of the (a) CCA applicator (b) CCB applicator in the water phantom.

Table 3: Deposited energy in the eye components in MeV/g due to ^{106}Ru plaques.

Eye component	Deposited energy by per one particle of source (MeV/g)	
	CCA plaque	CCB plaque
Vitreous body	3.99965E-04 (1± 0.0051)	5.58321E-03 (1± 0.0049)
Retina	7.33090E-04 (1± 0.0036)	9.03942E-03 (1± 0.0033)
Choroid	1.73101E-03 (1± 0.0026)	2.47007E-02 (1± 0.0022)
Sclera	1.56826E-03 (1± 0.0027)	4.02129E-02 (1± 0.0018)
Tumour	1.79615E-01 (1± 0.0003)	1.06153E-01 (1± 0.0014)
Cornea	1.11082E-05 (1± 0.0291)	7.18254E-04 (1± 0.0124)
Anterior chamber	1.93096E-06 (1± 0.0686)	3.51933E-04 (1± 0.0207)
Lens	5.55507E-06 (1± 0.0393)	4.65551E-04 (1± 0.0175)

CONCLUSION

Dose deposition in high gradient region, near the source, can only be calculated accurately by Monte Carlo method. The result can be used in treatment planning systems and also for computation of model dependent parameters. The new model allows estimating doses to the tumor and to the healthy tissues for a conventional brachytherapy treatment with ^{106}Ru plaques. The calculated dosimetry parameters for the source are useful in treatment in therapeutic plan. The present work demonstrates a useful approach using MCNP code in dose calculation that can be applied in many other fields.

REFERENCES

1. Yazdani M, Mowlavi AA. Monte carlo dose distribution calculation of ^{131}Cs source in soft tissue phantoms using MCNP. Iran J Radiat Res 2007; 5(6): 47-52.
2. Lommatzsch P. Treatment of choroidal melanomas with ^{106}Ru/^{106}Rh beta ray applicators. Surv Ophthalmol 1974; 19(2): 85-100.
3. Lommatzsch P. Beta irradiation with ^{106}Ru/^{106}Rh applicators of choroidal melanomas: sixteen years experience. Fortschritte der Onkologie. Berlin: Akademic, 1983: 290-301.
4. Tjho-Heslinga RE, Kakebeeke-Kemme HM, Davelaar J, de Vroome H, Bleeker JC, Oosterhuis JA et-al. Results of ruthenium irradiation of uveal melanoma. Radiother Oncol 1993; 29(1): 33-38.
5. Cross WG, Hokkanen J, Järvinen H, Mourtada F, Sipilä P, Soares CG et al. Calculation of beta-ray dose distributions from ophthalmic applicators and comparison with measurements in a model eye. Med Phys 2001; 28(7): 1385-1396.
6. Chiu-Tsao ST, Anderson LL, O'Brien K, Stabile L, Liu JC. Dosimetry for ^{125}I seed (model 6711) in eye plaques. Med Phys 1993; 20(2): 383-389.
7. Yoriyaz H, Sanchez A, dos Santos A. A new human eye model for ophthalmic brachytherapy dosimetry. Radiat Prot Dosimetry 2005; 115(1-4): 316-319.
8. Briesmeister JF. MCNP- A general Monte Carlo N-particle transport code, version 4C. Los Alamos National Laboratory Report LA-13709-M, 2000.
9. ICRP Report 38. Radionuclide transformations: energy and intensity of emissions. Oxford: Pergamon Press, 1983.
10. Sánchez-Reyes A, Tello JI, Guix B, Salvat F. Monte Carlo calculation of the dose distributions of two ^{106}Ru eye applicators. Radiother Oncol 1998; 49(2):191-196.
11. International commission on radiological protection. Report of the task group on reference man. ICRP Report 23, Oxford: Pergamon Press, 1975.

12. Gleckler M, Valentine JD, Silberstein EB. Calculating lens dose and surface dose rates from ^{90}Sr ophthalmic applicators using Monte Carlo modeling. Med Phys 1998; 25(1): 29–36.
13. Stallard HB. Radiotherapy for malignant melanoma of the choroid. Br J Ophthalmol 1966; 50(3): 147–155.
14. Howarth C, Meyer D, Hustu HO, Johnson WW, Shanks E, Pratt C. Stage-related combined modality treatment of retinoblastoma. Cancer 1980; 45(5): 851–858.
15. McCormick B, Ellsworth R, Abramson D, Haik B, Tome M, Grabowski E et al. Radiation therapy for retinoblastoma: comparison of results with lens-sparing versus lateral beam techniques. Int J Radiat Oncol Biol Phys 1988; 15(3): 567–574.
16. Shields JA, Augsburger JJ, Brady LW, Day JL. Cobalt plaque therapy of posterior uveal melanomas. Ophthalmology 1982; 89(10):1201-1207.
17. Gagnon JD, Ware CM, Moss WT, Stevens KR. Radiation management of bilateral retinoblastoma: the need to preserve vision. Int J Radiat Oncol Biol Phys 1980; 6(6): 669–673.
18. Jarrett JM. Experimental method development for permanent interstitial prostate brachytherapy implants. MSc Thesis in Southeastern Louisiana University, 2005.